J. Physiol. (1978), **281**, *pp.* 77–99
With 10 *text-figures*
Printed in Great Britain

INACTIVATION KINETICS AND STEADY-STATE CURRENT NOISE IN THE ANOMALOUS RECTIFIER OF TUNICATE EGG CELL MEMBRANES

BY HARUNORI OHMORI

From the Department of Neurophysiology, Institute of Brain Research, School of Medicine, University of Tokyo, Tokyo, Japan

(*Received 14 June 1977*)

SUMMARY

1. Inward K current through the anomalous rectifier in the tunicate egg (*Halocynthia roretzi*, Drashe) was studied under voltage clamp. The transient inward current in response to a step change of membrane potential was measured. The steady-state current fluctuations were analysed using the power density spectrum (p.d.s.).

2. The inward current showed time-dependent changes, which were described by a pair of first order kinetic parameters, n and s for activation and inactivation, respectively. The steady-state channel open probability due to the activation process (n_∞) was assumed to be 1·0 for V more negative than about -100 mV, but that of the inactivation process (s_∞) and the time constant of inactivation (τ_s) were membrane potential dependent in the same potential range; both decreased with increasing hyperpolarization.

3. The inward currents in Na-free choline medium did not inactivate, but were decreased in size. In Na-free Li medium, inactivation was very small; the steady-state conductance was not affected significantly.

4. After exposure to high Ca media, an increase of the conductance was observed. This effect is probably caused by an increase of intracellular Ca due to Ca ions entering through the Na channels. Mg ions slightly decreased the conductance.

5. In the hyperpolarized membrane ($-160 \leqslant V \leqslant -80$ mV), steady-state current noise was recorded and analysed using p.d.s. A p.d.s. of the $1/[1+(f/f_c)^2]$ type as well as a p.d.s. of the $1/f$ type was observed; f, frequency, f_c, cut-off frequency.

6. f_c was translated into time constant τ_N ($= 1/2\pi f_c$) and compared with the time constant of inactivation, τ_s. There was a significant correlation between these values, with a regression coefficient of 0·82.

7. Changing from 400 mM-Na to 400 mM-Li abolished inactivation and changed the p.d.s. from the $1/[1+(f/f_c)^2]$ into the $1/f$ type. These results (paragraphs 5–7) suggest that the fluctuations in the steady-state currents originate in the inactivation gating kinetics of the anomalous rectifier.

8. The number of anomalous rectifier channels and the unit channel conductance were estimated from the $1/[1+(f/f_c)^2]$ type current noise according to the formula

$$S(f) = \frac{2I_\infty^2(1-s_\infty)\tau_s}{s_\infty N[1+(2\pi f\tau_s)^2]},$$

where $I_\infty = \gamma N n_\infty s_\infty (V-V_K)$, γ the unit channel conductance, N the maximum number of channels that can be opened by a hyperpolarizing pulse per egg. The unit

conductance was 6 pmho in standard artificial sea water and the channel density was $0{\cdot}028/\mu m^2$.

9. The unit channel conductance (γ) was dependent upon external K concentration, but the number of channels (N) was not.

10. The increase in chord conductance evoked by higher Ca concentrations was due to the increase of the channel number. By contrast, Mg ions seem to decrease the unit channel conductance slightly.

INTRODUCTION

Anomalous rectification which has been found in the frog muscle membrane (Katz, 1949; Adrian & Freygang, 1962) is present in the egg cell membrane of the tunicate and the starfish (Okamoto, Takahashi & Yoshii, 1976*a*; Hagiwara, Miyazaki & Rosenthal, 1976). The K inward current through the rectifier shows fast activation and later slow inactivation in response to a hyperpolarizing step change of membrane potential. The activation process is too fast for quantitative analysis in the tunicate; only in the starfish egg membrane it has been analysed in detail (Hagiwara *et al.* 1976). Slow inactivation of the inward K current has also been observed in frog muscle and studied quantitatively by the voltage-clamp technique (Almers, 1972*a*, *b*).

In the present experiments the slow inactivation of the anomalous rectifier in the tunicate egg will be described quantitatively both by macroscopic analysis of the transient inward current associated with step changes of membrane potential and by microscopic analysis of steady-state current fluctuations. In addition, the study of the steady-state current fluctuations allow determination of the number and the unit conductance of the anomalous rectifier channels in the egg membrane.

METHODS

Preparations. Unfertilized eggs of the tunicate *Halocynthia roretzi* Drashe, with a mean diameter of 270 μm, were used. The follicular envelope covering the egg was unwrapped manually with a pair of fine needles under a binocular microscope or was digested by the enzyme *pronase*. The denuded egg was transported into a bathing chamber made of Lucite, and placed in a shallow small hole at the bottom. The temperature of the chamber was regulated by Peltier thermoplates (see Miyazaki, Takahashi & Tsuda, 1974*a*). The temperature was kept at 15 °C in most experiments.

Solutions. As a standard solution 50 mM-KCl, 210 mM-NaCl, 10 mM-$CaCl_2$, and 285 mM-choline Cl was used. Other solutions used are listed in Table 1. The pH of the solutions was adjusted to 7·6 with Tris-Cl (10 mM). In solutions F, G and H, PIPES-K (10 mM, pH = 6·9) was used instead of Tris-Cl.

Recording and experimental procedures. All experiments were done by using the voltage-clamp technique with two glass micro-electrodes filled with 3 M-KCl, having 3–5 MΩ resistance. One electrode was used for potential recording and the other for current injection. A precise description of the circuit and the accuracy of current measurements is given in a previous paper (Okamoto *et al.* 1976*a*). As shown in Fig. 1 the output signals of preamplifiers both for membrane current and for membrane potential were sampled and memorized transiently (Kawasaki Electronica TM 1510, 8 bits 1024 words), and reproduced at a slower rate on a high speed multichannel pen recorder (Rikadenki B-26 Mark II). For current noise analysis 2 min samples of the membrane current were recorded with an FM magnetic tape data recorder (TEAC R410).

As shown in Fig. 1, high frequency components of membrane current were filtered out using the low pass filter-1 (6 dB/octave, at 300 or 800 Hz) before the input of the transient memory. The filtered current signals, amplified 10 times, were fed to the data recorder through the low pass filter-2, 12 dB/octave roll off at 100 Hz. The current noise records in the data recorder

were reproduced, amplified 20 times, and fed to an A/D converter (10 bits) of a computer (TOSBAC 3400) through the low pass filter-3, 18 dB/octave roll off at 80 Hz, to prevent aliasing. The frequency response of the total recording system was flat from d.c. to more than 50 Hz.

In the beginning of each experiment, the membrane potential was held at zero current level. It was changed stepwise by hyperpolarizing pulses and inward going transient currents were recorded. This procedure will be called a relaxational voltage-clamp run. After a series of relaxational runs, the holding potential was changed to a more hyperpolarized level to record steady-state current noise. Current noise at several levels of membrane potentials was recorded

TABLE 1. Ionic composition of the artificial sea waters (mM)

Soln.	KCl	NaCl	LiCl	Choline-Cl	$CaCl_2$	$MgCl_2$
A	300	210	—	35	10	—
B	—	210	—	335	10	—
C	50	210	—	—	200	—
D	50	210	—	—	—	200
E	50	210	—	300	—	—
F	50	400	—	95	10	—
G	50	—	400	95	10	—
H	50	—	—	495	10	—

10 mM Tris-Cl (pH = 7·6) or 10 mM-PIPES-K (pH = 6·9) was added to the solutions. Intermediate concentrations of K, Ca or Na were obtained by mixing solutions A and B, C and E or F and H, respectively.

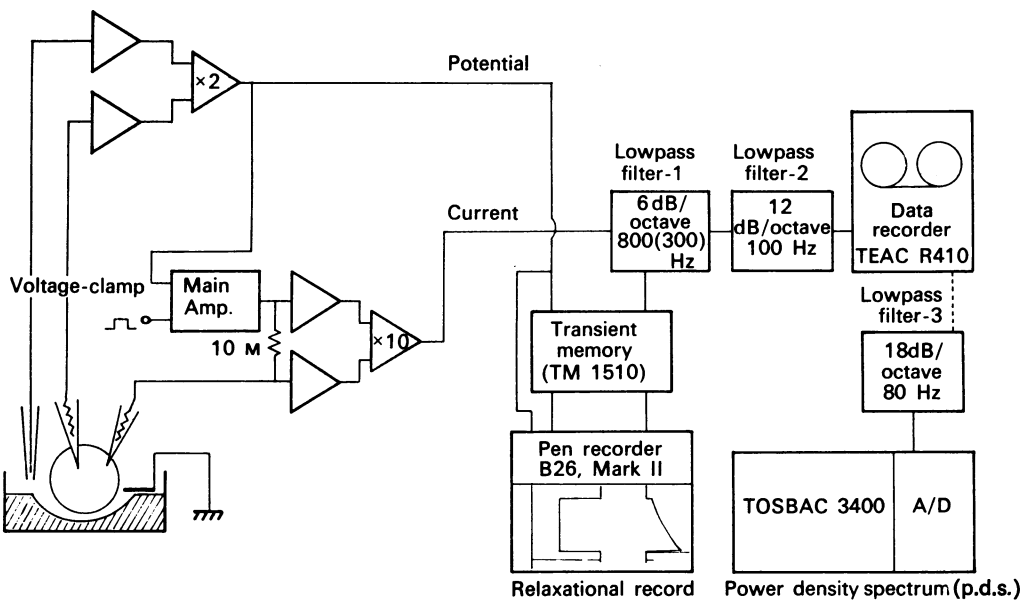

Fig. 1. Circuit and block diagram of voltage-clamp recording system and computer analysing system of steady-state current noise.

on the magnetic tape, usually from −80 to −160 mV with 20 mV intervals and from −150 to −110 or −90 mV with the same intervals. After completion of the current noise recordings, the holding potential was returned to the level of zero current potential and relaxational voltage-clamp runs were again made. After these three procedures, the external solution was changed and the next experiment was started. At the end of a series of experiments the external solution was changed to K-free medium to detect the amount of leakage currents.

Data processing. Current noise recorded on the FM data recorder was reproduced and a p.d.s., $S(f)$, was estimated by the computer. The steady-state current noise was fed to the A/D

converter, sampled uniformly at 9·8 msec intervals, and assembled into 10 data blocks of 1024 digital points. Records of 100 sec were used for spectral analysis. The sampled records were transformed to a set of frequency components using fast Fourier transformation and the power density spectrum was estimated as the squared values of the amplitudes of each frequency component. Each data block was independently analysed and the values from 10 data blocks were finally averaged. The final spectrum consisted of 512 points, 0·1 Hz apart from 0·1 to 51 Hz. The standard deviation of the spectral estimation is $S(f)/\sqrt{BT} = 0{\cdot}3\,S(f)$, where B is the frequency resolution and T is the total recording period (Bendat & Piersol, 1971). The spectrum and formula used in this paper are for a 'two sided' power density spectrum (Bendat & Piersol, 1971), and only the positive frequency side of the spectrum was used.

At about 50 Hz, a sharp peak was always detected in p.d.s., caused by the 50 Hz alternating current power supply, and was used as a frequency calibration.

System noise. Noise generated by the recording system and the resting membrane was also analysed, holding the membrane potential at zero current level. The power of such system noise was almost constant from 0·1 to 20 Hz and increased gradually above 20 Hz. The power in the lower frequency region was lower than 2×10^{-25} A² sec and it stayed below 5×10^{-25} A² sec up to 50 Hz. The system noise in the lower frequency region was generally 2 orders of magnitude less than the current noise reported in Results.

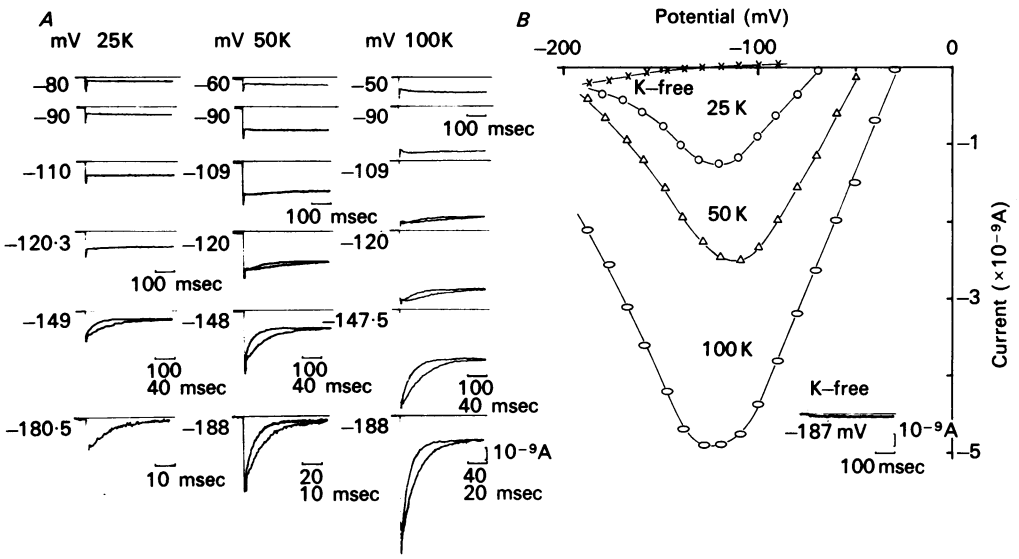

Fig. 2. Steady-state I–V relations and traces of inward current. A, traces of inward current in 25, 50 and 100 mM-K solutions. In some of the records, two traces with a fast and a slow sweep speed were superimposed to show the steady state level of the current. Except for the bottom traces in each column, the calibration is 100 msec and 40 msec for slower and faster time base, respectively. B, steady-state I–V relations; K-free (×), 25 mM-K (○), 50 mM-K (△) and 100 mM-K (oval). The membrane potential was held at −100 (K-free), −70 (25 mM-K), −50 (50 mM-K) and −30 (100 mM-K) (mV), and was hyperpolarized stepwise to the levels indicated. Inset shows a trace of current in K-free medium. Solutions A and B.

RESULTS

Part I. Properties of anomalous rectification in the egg cell membrane

The current through the anomalous rectifier. In solutions containing K ions, the inward current associated with hyperpolarizing pulses showed an instantaneous rise which, for strong pulses, was followed by slow inactivation (Fig. 2A). After the slow

inactivation, a steady state was reached. The holding potential was set at zero membrane current in each medium. In Fig. 2*B* the steady-state currents are plotted against the membrane potential for four different K concentrations (0, 25, 50 and 100 mM-K). The *I–V* relations have a negative slope at potentials more negative than about −120 mV, corresponding to the appearance of the inactivation of the inward currents.

Fig. 2*B* (inset) shows that the inward current became negligible in K-free medium. When the choline ions in the K-free medium were replaced with Li, Na or Cs, the inward current was also negligible. Although small inward currents were observed in these K-free media in the highly hyperpolarized membrane, these non-K or leakage currents showed no time-dependent component and were almost ohmic in character (Figs. 2*B*, 4*B*, 4*D*).

The intracellular K concentration $[K]_i$ was estimated from the resting potentials in Na-free high K solution (100, 200 and 300 mM) by using the Nernst equation. The estimated $[K]_i$ ranged from 233 to 291 mM; the average 260 mM will be used for calculation of V_K later. The $[K]_i$ is larger than the value 204 mM estimated previously for the eggs of the tunicate *Halocynthia aurantium* (Miyazaki *et al.* 1974*a*). The difference may reflect a species difference.

Kinetic properties of the K inward current. The kinetics of the K inward current were analysed quantitatively according to the method of Hodgkin & Huxley (1952). In Fig. 3*A* such an analysis is illustrated for step changes of potential from −50 to −109, −140, −157 and −177 mV in 50 mM-K solution. The current rose instantaneously; a further small rise was visible at small pulse heights (see Fig. 2*A*, 100 mM-K, −90, −109, −120 mV). With strong hyperpolarizing pulses a marked inactivation was seen. The difference between the current at time t, $I(t)$, and the steady value, I_∞, indicated by the superimposed record with the slower sweep speed, was plotted against time semilogarithmically; the decay phase was linear as illustrated in Fig. 3*A*.

Using n as activation parameter and s as inactivation parameter, the inward current $I(t)$ can be formulated as

$$I(t) = \bar{g}ns(V - V_K), \tag{1}$$

where $\bar{g}$ is the maximum chord conductance of the K channel, V the membrane potential and V_K the K equilibrium potential. The product ns indicates the open probability of the K channel and both n and s vary independently from 0 to 1. Activation was so fast that a precise analysis was impossible. Therefore, the activation process was presumed to follow first order kinetics as observed in the starfish egg membrane (Hagiwara *et al.* 1976). Under this assumption n and s can be described as follows;

$$n = n_\infty + (n_0 - n_\infty)\, e^{-t/\tau_n}, \tag{2}$$

$$s = s_\infty + (s_0 - s_\infty)\, e^{-t/\tau_s}, \tag{3}$$

where (0) and (∞) indicate the initial and final states τ_n and τ_s are the time constants of activation and inactivation, respectively. n_∞ and s_∞, τ_n and τ_s are dependent upon the membrane potential V, while n_0 and s_0 depend only upon the holding potential and are taken as constants.

The values of n_∞ were inferred indirectly using zero-time extrapolated values of

the decaying phase of the inward current. Defining $\Delta I^*(t)$ as a regression line of $\Delta I(t) = I(t) - I_\infty$ in Fig. 3*A*, it is deduced that

$$I^*(t) = \Delta I^*(t) + I_\infty$$
$$= \bar{g} n_\infty (s_\infty + (s_0 - s_\infty)\, e^{-t/\tau_s}) (V - V_K) \qquad (4)$$

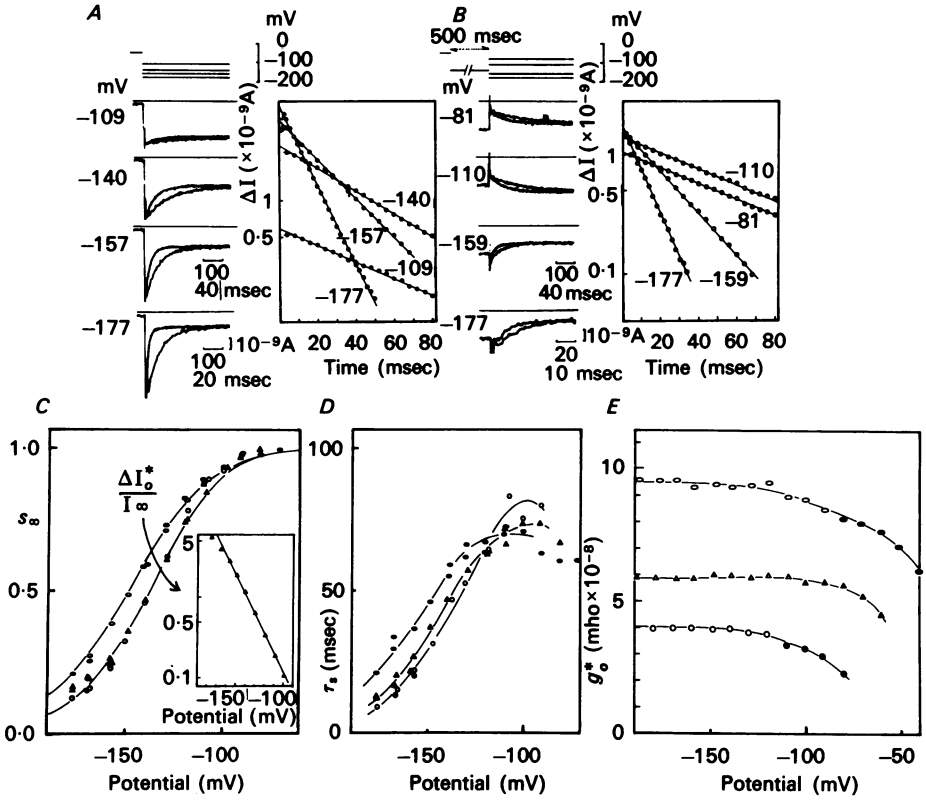

Fig. 3. Graphical analysis of inward currents. *A*, traces of inward currents in response to a single step hyperpolarizing pulse from −50 mV in 50 mM-K standard solution. *B*, traces of inward currents in response to a test pulse after a 500 msec hyperpolarizing prepulse to −140 mV in 50 mM-K standard solution. In *A* and *B*, transient components of each inward currents ($\Delta I = I(t) - I_\infty$) were plotted on log scale against time. *C*, *D*, membrane potential and external K concentration (○, 25 mM-K; △, 50 mM-K; oval, 100 mM-K) dependent changes of s_∞ and τ_s. Inset in 3*C* shows the ratios $\Delta I_0^*/I_\infty$ (50 mM-K) plotted on log scale against potential. Open symbols were obtained from currents recorded with single step potential pulses. Filled symbols were obtained from records with a hyperpolarizing prepulse of 500 msec duration to −140 mV (25, 50 mM-K) or to −150 mV (100 mM-K). In 3*C*, and successive Figures, the continuous curves for s_∞-potential were drawn according to eqn. (5). Details are in Results. V_s = −138 (25, 50 mM-K), −149 (100 mM-K), b = 19 (25, 50 mM-K), 22 (100 mM-K) (mV). In 3*D*, and successive Figures, the smooth curves for τ_s-potential were drawn through the experimental points by eye. *E*, zero-time extrapolated chord conductance plotted against membrane potential. At the membrane potentials where no inactivation was observed, the steady-state conductance was plotted (filled symbols) instead of zero-time extrapolated values. Symbols are the same for *C*, *D* and *E*. Solutions *A* and *B*.

and the zero-time value I_0^* is $\bar{g}n_\infty s_0(V-V_K)$. Therefore, the zero-time extrapolated value of the conductance (g_0^*) is $\bar{g}n_\infty s_0$, which is plotted against membrane potential in Fig. 3*E*, for 25 (○, ●) 50 (△, ▲) and 100 mM-K (oval) in the standard solution. The smooth curves were drawn through the experimental points by eye. g_0^* values are almost constant at large hyperpolarized potentials, irrespective of K concentration. Therefore, the product $n_\infty s_0$ should be constant in the membrane potential range where g_0^* is constant. As s_0 is constant, n_∞ must be constant. Thus, n_∞ can be assumed as 1·0 at potentials more negative than about −100 mV, especially for 50 mM-K media. It is known that the instantaneous chord conductance of the anomalous rectifier changes significantly with the driving force, $(V-V_K)$ (Hagiwara *et al.* 1976). Therefore, the decrease of g_0^* at potentials more positive than about −100 mV may be due to a decrease in $\bar{g}$, in addition to the change in n_∞.

The parameters of the inactivation process were estimated from semilogarithmic plots of $\Delta I(t)$ against time. Since $I_\infty = \bar{g}n_\infty s_\infty(V-V_K)$, and $I_0^* = \bar{g}n_\infty s_0(V-V_K)$, I_∞/I_0^* is s_∞/s_0. For example in the case of Fig. 3*A*, assuming no inactivation at the holding level of −50 mV, i.e. $s_0 = 1{\cdot}0$, s_∞ at −140 mV was calculated as 0·45. Since $\bar{g}$ is considered to be a time invariant parameter, the time constant of the decay phase of the inward current directly corresponds to τ_s. s_∞ and τ_s, thus calculated for the various membrane potentials and for the various K solutions, are plotted against potential in Fig. 3*C*, *D*, respectively.

At potentials where inactivation is small, the estimation of s_∞ and τ_s by the method described above becomes inaccurate. To overcome this difficulty a hyperpolarizing prepulse to a potential at which pronounced inactivation occurs was used. Kinetic parameters s_∞ and τ_s (filled symbols in Fig. 3*C*, *D*) were determined by the use of a 500 msec hyperpolarizing prepulse to −140 mV (25, 50 mM-K) or to −150 mV (100 mM-K). Fig. 3*B* shows traces of inward current after a prepulse to −140 mV in 50 mM-K solution and semilogarithmic plots of $\Delta I(t)$ against time. The time course of $\Delta I(t)$ was exponential. s_∞ and τ_s estimated with prepulse (filled symbols) coincided with those estimated without prepulse (open symbols) (Fig. 3*C*, *D*). These results suggest that there is no change in the activation state from −140 to −81 mV and that the steady-state activation (n_∞) is saturated and probably 1·0 for the potential of −81 mV. This result, thus, supports the suggestion that n_∞ is constant in these potential ranges, as was described above (Fig. 3*E*).

The relation between s_∞ and membrane potential was examined in the following way. The ratios between the zero-time extrapolated value of the regression line $\Delta I^*(t)$ and I_∞, $\Delta I_0^*/I_\infty = (1-s_\infty)/s_\infty$ (in 50 mM-K solution) were plotted semilogarithmically against potential (Fig. 3*C* inset). Except for the ratios at potentials more negative than −160 mV and around −100 mV, the values fell on a straight line. Therefore, the relation between s_∞ and potential can be described by the equation

$$s_\infty = \frac{1}{1+\exp\left[-(V-V_s)/b\right]}, \tag{5}$$

where V_s is the membrane potential at which inactivation becomes half ($s_\infty = 0{\cdot}5$) and b is a constant determining the maximum slope of the curve. V_s and b were estimated by least squares from the data points in the potential range between

-100 and -160 mV. In Fig. 3*C*, b was 19, 19, 22 mV and V_s was -138, -138, -149 mV in 25, 50 and 100 mM-K solutions, respectively.

Although the leakage current or non-K current is very small as shown in Fig. 2*B*, it can induce an apparent increase in s_∞, especially at the membrane potentials more negative than -160 mV. Actually in this potential range, systematic deviations from the s_∞-potential curves drawn from eqn. (5) were observed (Figs. 3*C*, 5*D*, 9*A*). The deviation around -100 mV was probably due to underestimation of the small transient portion of the current. By the use of hyperpolarizing prepulses, the estimation of parameters around -100 mV became more precise (Fig. 3*B*), but the procedure frequently led to deterioration of the membrane. Therefore, in the later experiments, s_∞ and τ_s were estimated from the current traces associated with single step potential pulses. The curves in the s_∞-potential diagrams were drawn by using eqn. (5) and the parameters of V_s and b estimated from semilogarithmic plots of $\Delta I_0^*/I_\infty$ against potential in the range -160 to -100 mV. The τ_s-potential relations were drawn through the experimental points by eye and were similar to those for s_∞. Both curves were dependent upon K concentration: they shifted in a hyperpolarized direction and became less steep as the external K concentration increased.

The time constant of inactivation (τ_s) was found to be temperature-dependent as it is in other ionic channels. Q_{10} of τ_s was 3·41 in the temperature range from 5 to 20 °C. The activation energy was estimated to be about 20 kcal/mol which is the same as that of the time constants of activation or inactivation of Na channels in the tunicate egg (Okamoto *et al.* 1976). The temperature coefficient of the chord conductance was 1·44. This was similar to that observed for the Na channel in the tunicate egg.

Na ions as inactivators of the K inward current through the anomalous rectifier channel. In myelinated nerve fibres (Bergman, 1970) and squid giant axons (Bezanilla & Armstrong, 1972), internal Na ions are known to inactivate the K outward current through the delayed rectification channel, especially for large positive membrane potentials. K inward current through the anomalous rectifier in the tunicate egg was inactivated in the range of large negative membrane potentials, and a negative conductance in the steady-state I–V relations was observed (Figs. 2*B*, 4*B*, *D*.) Since the external medium always contained Na ions, it is possible that external Na ions inactivate K inward currents and cause the negative conductance region in the I–V relation.

In Fig. 4*A*, K inward currents in Na-free standard solution are illustrated. The inward currents show time-dependent activation (arrow in Fig. 4*A*, Na-free), but even at a potential of -184 mV no inactivation was observed. Although the inward going rectifier was still present in Na-free solution, a negative conductance in the steady state I–V relation was not found (Fig. 4*B*). These changes in the inactivation process were completely reversible; by raising the Na concentration to 400 mM, the potential dependent inactivation as well as the negative conductance appeared again as shown in Fig. 4*A*, *B*. In 400 mM-Li, Na-free solution, inactivation occurred only at potentials more negative than -160 mV (Fig. 4*C*).

The chord conductance in the positive slope region of the I–V relation decreased in Na-free choline solution (Fig. 4*B*). While a further reduction in the conductance was observed after replacement of choline with TEA (tetraethylammonium-Cl),

replacement of choline with TMA (tetramethylammonium-Cl) or with isomolar glucose had no effect upon the chord conductance in Na-free media. The steady-state conductance in Na-free Li medium was similar to or larger than that in 400 mM-Na (Fig. 4*C*, *D*). Na ions as well as Li ions seem to exert facilitating effects upon the channel conductance, in addition to the inactivating effect upon the channel.

In 400 mM-Na, K-free medium, the amount of steady current was negligible (Fig. 4*B*, inset). Li ions did not permeate through the anomalous rectifier channel (Fig. 4*D*, inset). Therefore, Na and Li ions seem to modify the conductance of the anomalous rectifier channel, although they can not permeate through the channel.

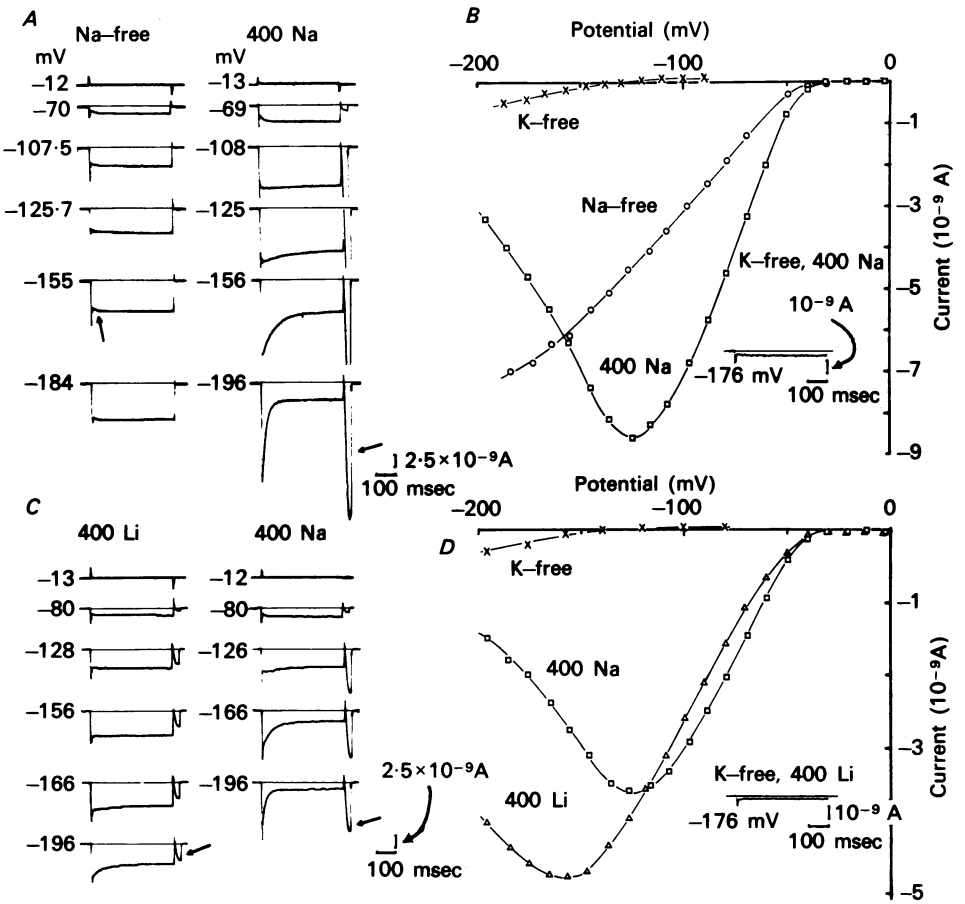

Fig. 4. Inactivating effect of Na ions. *A*, traces of inward current in Na-free choline and in 400 mM-Na solution. In Na-free solution, only activation was observed (arrow). Note Na inward current through the Na channel at end of hyperpolarizing test pulse (4*A*, *C*, 400 Na, arrows). *B*, steady-state *I–V* relations for the inward currents in *A*. Note disappearance of the negative slope region in Na-free solution. Inset shows record in 400 mM-Na, K-free solution. *C*, traces of inward current in Na-free, 400 mM-Li and in 400 mM-Na solution. In 400 mM-Li solution, inactivation was observed only at potentials more negative than about −160 mV. Note Li current through the Na channel after the hyperpolarizing pulse (400 Li arrow). *D*, steady state *I–V* relations for the inward currents in *C*. Inset shows current in 400 mM-Li, K-free solution. Solutions F, G and H.

Ca and Mg effects upon the K anomalous rectifier channel. Divalent cations such as Ca^{2+} had no effect upon the inactivation of the anomalous rectifier when their concentration was changed from 10 to 50 and then to 200 mM (Fig. 5*D*). The steady-state *I–V* relations for the same experiment are illustrated in Fig. 5*A*. In the *I–V* relations an increase of the chord conductance was observed with increasing Ca

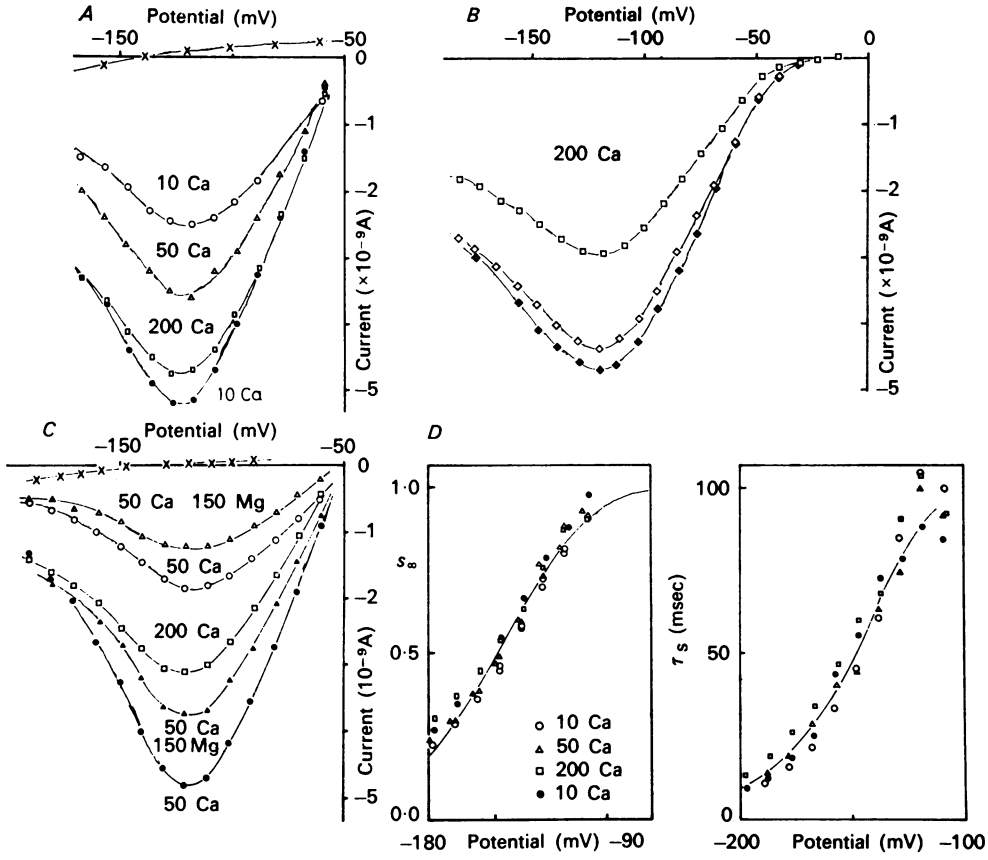

Fig. 5. Changes in steady-state *I–V* relations and s_∞- and τ_s-potential curves with divalent cation concentration (mM) changes. *A*, Ca concentration changed from 10 (○) to 50 (△), then to 200 (□) and again to 10 (●). Membrane potential held at −50 mV. Solutions C and E. *B*, steady-state *I–V* relations in 200 Ca solution. Membrane potential held at −90 mV (□) or at −40 mV (◇, ◆). *I–V* relation represented by ◆ was obtained with depolarizing prepulses of 1 sec duration to +27 mV. Solution C. *C*, Ca concentration changed, keeping total divalent cationic concentration constant ([Ca]+[Mg] = 200 mM). *I–V* relation in 50 Ca solution without Mg also included. Filled symbols show measurements after 200 Ca bath. In *A* and *C* (×) denotes records in K-free media. Solutions C, D and E. *D*, s_∞- and τ_s-potential curves obtained from the records in *A*. $V_s = -149$ mV, $b = 20$ mV.

concentration. The conductance remained high when changing back from 200 to 10 mM-Ca (filled circles in Fig. 5*A*). The conductance in 10 mM-Ca increased 1·8 times after bathing the egg in 200 mM-Ca solution (Fig. 5*A*); the conductance in

50 mM-Ca also increased after equilibrating with 200 mM-Ca (Fig. 5*C*, filled circles). The potential at which the inward currents became maximum remained unchanged when changing the Ca concentration.

In the egg cell membrane of the tunicate extracellular Ca ions modify reversibly the conductance of the Na and Ca channels through their effects upon the negative surface charges (Ohmori & Yoshii, 1977). In contrast to the effects upon Na and Ca channels, the extracellular Ca ions did not change the membrane potential dependency of s_∞ and τ_s and only a conductance increase was observed after increasing the extracellular Ca concentration. The effect of Ca ions on the anomalous rectifier is to modify the chord conductance of the channel.

A similar increase of K conductance related to Ca ions has been reported in other excitable membranes (Krnjević & Lisiewicz, 1972; Isenberg, 1975). In those cases ionized intracellular Ca has been thought to be important for the modification of the conductance. In *Helix aspersa* neurones, Meech & Standen (1975) have observed a Ca sensitive delayed increase in K conductance and have suggested that the increase is due to the direct action of intracellular Ca ions entered through the late Ca channels which have been found in squid giant axons (Baker, Hodgkin & Ridgway, 1971).

There are two pathways for the influx of Ca ions in the egg cell membrane of the tunicate, Na and Ca channels (Okamoto *et al.* 1976*b*). The Na channel seems to be more important as influx pathway for Ca ions which influence the anomalous rectifier. Because a hyperpolarizing prepulse of 400 msec duration beyond -90 mV is sufficient to remove the steady-state inactivation of the Na channel (Okamoto *et al.* 1976*a*), there is a possibility that, together with Na ions, small amounts of Ca ions enter the intracellular compartment through the Na channel when the membrane potential is returned to the holding level of -50 mV after the 400 msec hyperpolarizing pulses which are used for inducing K inward current through the anomalous rectifier (Fig. 4*A*, *C*, 400 mM-Na, arrow). In order to block this influx of Ca ions, the holding potential must be more negative than -90 mV so that the Na channel is not activated. When the holding potential was -90 mV initially in a 200 mM-Ca solution and then changed to -40 mV, the steady-state chord conductance increased significantly (Fig. 5*B*). The ratio of conductance measured at a holding level of -40 mV (◇) to that at -90 mV (□) was 1·55.

On the other hand, Ca channels will be opened by depolarizations to positive potentials. There was a slight further increase in the steady-state conductance of the anomalous rectifier (◆) when a depolarizing prepulse of 1 sec duration to $+27$ mV, where Ca inward current is maximum in a 200 mM-Ca solution, preceded the hyperpolarizing test pulse from the holding level of -40 mV. The ratio between the conductances with and without depolarizing prepulse was 1·14. The effect may be due to the influx of Ca ions mainly through Ca channels during the depolarizing prepulses.

Conductance changes related to the holding potential or to preceding depolarizing pulses were also observed in low Ca medium (10 mM) although to a lesser degree. The results suggest that the conductance enhancement associated with the increase of external Ca concentration is probably due to the action of intracellular Ca ions.

The presence of Mg ions also had no effect upon the potential dependency of the

inactivation process. In contrast to Ca, addition of Mg ions reduced the steady-state conductance although the effect was small (Fig. 5*C*).

Part II. Current noise analysis and identification of the origin of the noise

In part I, properties of the inactivation process of the anomalous rectifier channel were presented. Inactivation was analysed assuming first order kinetics. In part II, the steady-state current noise will be examined at various levels of membrane potential by using Fourier analysis.

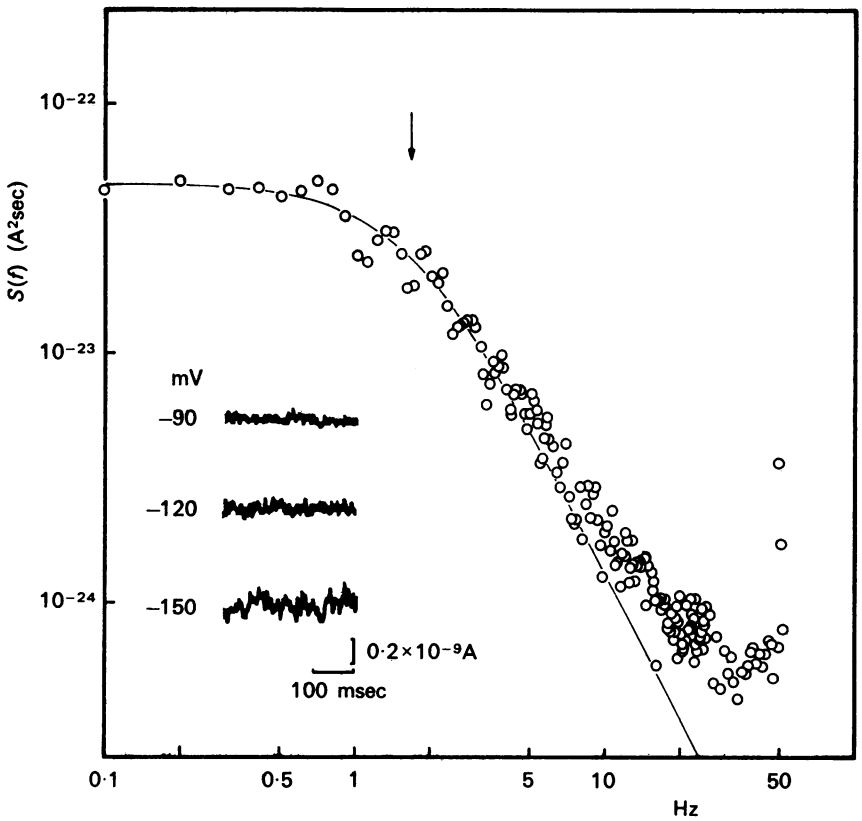

Fig. 6. Steady-state current noise and power density spectrum, p.d.s. Steady-state current noise was recorded at −90, −120 and −150 mV (inset). Steady-state current noise at −120 mV was decomposed into frequency domain and is presented in p.d.s. form. Ordinate is power (A^2 sec), abscissa is frequency, both on log scale. Arrow indicates the cut-off frequency (f_c). Continuous curve was drawn according to eqn. (7); $I_\infty = -2{\cdot}2$ nA, $V = -120$ mV, $s_\infty = 0{\cdot}76$, $f_c = 1{\cdot}67$ Hz, $\gamma = 6{\cdot}0$ pmho, $N = 5930$. Solutions A and B (50 mM-K).

Fluctuation of membrane current at the steady state. When the holding potential was shifted from V_K to a more hyperpolarized level, the current noise superimposed upon the steady current was markedly enhanced as shown in Fig. 6, inset. These current noises were transformed into the frequency domain by using the fast Fourier transformation as described in Methods. The squared amplitudes of respective frequency components were plotted against the frequency in log–log co-ordinate as in Fig. 6.

This is the p.d.s. of the steady-state current noise at −120 mV. The spectral densities were almost constant in the low frequency range (less than 1 Hz) and approached a slope proportional to $1/f^2$ in the high frequency range (more than 3 Hz) except for a slight deviation at frequencies above 10 Hz. This deviation in the higher frequency region was mostly due to the additional power originating in the recording system (see Methods, system noise), and the sharp peak at about 50 Hz was due to 50 Hz from the power supply. The p.d.s. of the steady-state current noise had essentially a $1/[1+(f/f_c)^2]$ pattern. The arrow indicates the cut-off frequency (f_c) at 1·67 Hz at which the power becomes half of the low frequency asymptotic value.

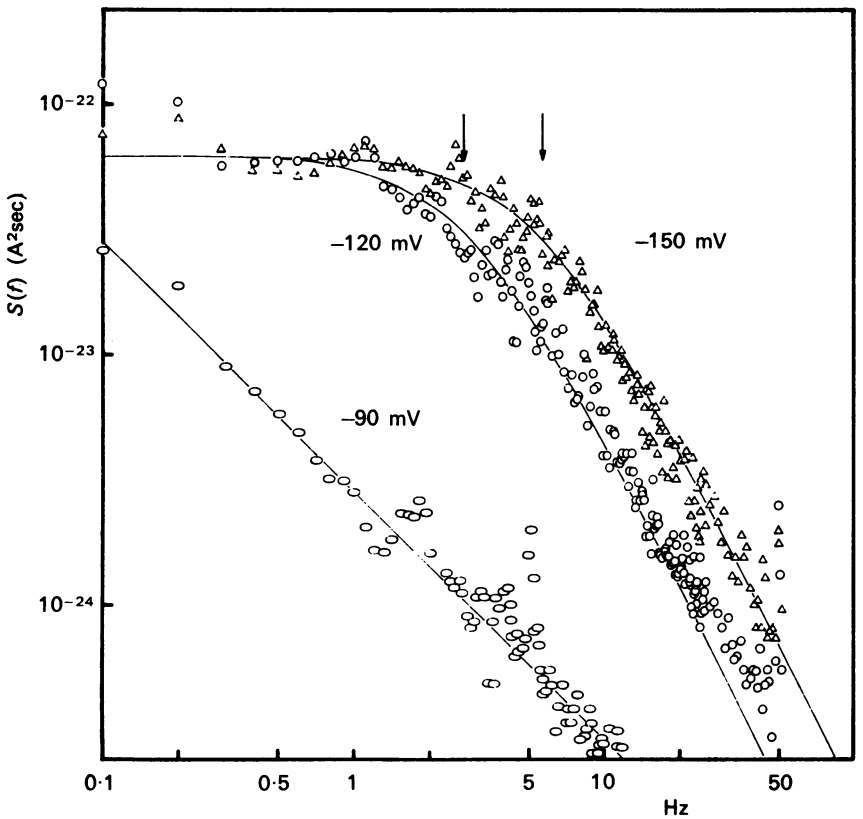

Fig. 7. Power density spectrum of steady state current noise at −90, −120 and −150 mV. Data points for −150 mV were multiplied by 0·72. For −120 mV, $I_\infty = -4{\cdot}0$ nA, $s_\infty = 0{\cdot}75$, $f_c = 2{\cdot}65$ Hz, $\gamma = 6{\cdot}5$ pmho, $N = 10300$. For −150 mV, $I_\infty = -3{\cdot}0$ nA, $s_\infty = 0{\cdot}39$, $f_c = 5{\cdot}31$ Hz, $\gamma = 7{\cdot}15$ pmho, $N = 9800$. p.d.s. at −90 mV showed the $1/f$ spectrum. Solution F.

The characteristic $1/[1+(f/f_c)^2]$ spectral pattern of electrical noise has been reported for several excitable membranes (Anderson & Stevens, 1973; Conti, De Felice & Wanke, 1975; Conti, Hille, Neumcke, Nonner & Stämpfli, 1976*a*, *b*). This pattern of the spectrum is related to the steady-state conductance fluctuations originating from the random movement of gating particles in each channel following a first order kinetic process.

The current noise spectra recorded at −90, −120 and −150 mV in another egg

cell membrane are shown in Fig. 7. The amplitude of the spectral density at -150 mV was multiplied by 0·72 for convenience of comparison on the frequency axis. The p.d.s. at -120 and -150 mV both showed a $1/[1+(f/f_c)^2]$ pattern, but the spectrum at -150 mV was clearly shifted to higher frequencies, the cut-off frequencies being 2·7 Hz at -120 mV and 5·3 Hz at -150 mV. The cut-off frequency in the spectrum can be transformed into a time constant by the formula:

$$\tau_N = 1/2\pi f_c. \tag{6}$$

In Fig. 7, time constants thus calculated were 60 and 30 msec at -120 and -150 mV, respectively. The time constants in the standard medium estimated from p.d.s. at various potential levels were plotted against membrane potential in Fig. 8*A*. The magnitude and the potential-dependency of τ_N were quite similar to those of τ_s, the

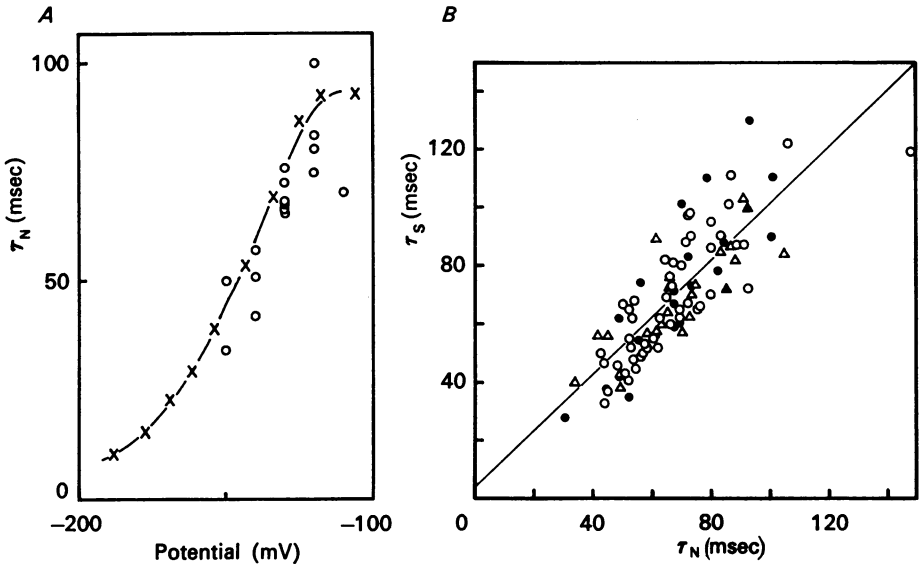

Fig. 8. The time constant calculated from noise analysis (τ_N) and correlation between τ_N and τ_s. *A*, τ_N-potential plot. τ_N was calculated from f_c in the power density spectrum by eqn. (6). Smooth curve was drawn through the average points of τ_s (marked with ×) estimated by relaxational voltage-clamp runs. Solutions A and B (50 mM-K). *B*, correlation diagram between τ_N and τ_s. Each τ_s was estimated in the same cell and at the same membrane potential where current noise recording for τ_N was made. Symbols indicate the experimental conditions when τ_N and τ_s were estimated. ○, substitution of Ca by Mg or by choline; solutions C, D and E. ●, substitution of Na by Li or by choline; solutions F, G and H. △, substitution of K by choline; solutions A and B. ▲, temperature changes; solutions A and B (50 mM-K). The straight line was $\tau_s = 0{\cdot}98\,\tau_N + 3{\cdot}41$ (regression coefficient = 0·82).

time constant of inactivation of the anomalous rectifier defined in part I. The continuous curve was drawn through the means (marked with ×) of τ_s values estimated by using step potential changes.

By making noise measurements between relaxational voltage-clamp runs, corresponding values of τ_s and τ_N were obtained and are plotted in Fig. 8*B* for eggs under various experimental conditions. The close correlation between the two kinds of time constant from various cells under various experimental conditions suggests that

the first order kinetics of the inactivation process is the origin of the current fluctuations represented by the $1/[1+(f/f_c)^2]$ patterned p.d.s.

Further identification of the origin of the current noise at the steady state. Besides the $1/[1+(f/f_c)^2]$ patterned spectrum presented in Figs. 6 and 7, a $1/f$ type of noise spectrum was frequently observed. The p.d.s. of the current noise at -90 mV in Fig. 7 is an example of such a spectrum. As shown in the current records from the relaxational voltage-clamp runs in Fig. 2*A*, 50 mM-K, the inward current at -90 mV did not inactivate. At the steady state the open probability of the channel due to an inactivation process was 1·0 as shown in Fig. 3*C*. The open probability of the channel due to the activation process was also assumed to be 1·0 around this potential in 50 mM-K solution (see p. 83). Thus, at the steady state at -90 mV, almost all channels are thought to be open and any microscopic open–close transition of the channels, if it occurred, would be very small in frequency. Therefore, it is reasonable that at -90 mV the current noise does not show the $1/[1+(f/f_c)^2]$ spectral pattern.

The $1/f$ spectrum has been observed not only in biological excitable membranes (Verveen & Derksen, 1965, 1968; Verveen & De Felice, 1974) but also in several physicochemical systems (Hooge & Gaal, 1971; Hooge, 1972). So far the power of the $1/f$ spectrum is known to be proportional to the squared values of the steady-state currents (Verveen & De Felice, 1974; Conti *et al.* 1975). Since this $1/f$ noise is thought to be independent of the fluctuation due to the gating kinetics, the two types of noise must additively contribute to the total power of the spectrum. Then, the upward deviation from the $1/[1+(f/f_c)^2]$ pattern sometimes observed in the lower frequency range at potentials from -120 to -150 mV would be partly due to this $1/f$ spectrum. The deviation in the lower frequency range could also be caused by non-stationary components of the current noise, since drifts of the macroscopic steady-state inward current should contribute to the p.d.s. as the low frequency power. The deviation varied considerably from cell to cell.

Data showing significant low-frequency deviation at $f > 0{\cdot}3$ Hz were discarded from further analysis. For the remaining data, which sometimes showed low frequency deviation at $f < 0{\cdot}3$ Hz, if the source of the deviation is assumed to be $1/f$ noise, the power of this noise is usually less than 1/10 of the total power, at least at the cut-off frequency.

Since the $1/[1+(f/f_c)^2]$ spectrum of the current noise is related to the open–close kinetics of the inactivation process and Na ions are thought to be inactivators of the K inward current as described in part I, a change in the spectral pattern should be observed in Na-free solution. Although inactivation was seen at potentials around -170 mV in 400 mM-Li, Na-free medium, inactivation did not occur at the potentials where noise recordings were made (-160 mV $\leqslant V \leqslant -80$ mV) and the steady-state conductance was not affected significantly by the replacement of external Na ions with Li ions (Fig. 4*C*, *D*). Therefore, it is possible to compare the spectrum of steady-state current noise recorded in the presence of inactivation (in 400 Na solution) and in the absence of inactivation (in 400 Li, Na-free solution) at the same membrane potential and with inward currents of similar size.

In Na-free Li medium, no inactivation occurred at -130 mV (Fig. 9*A*, inset). Therefore, the open probability of the channels at -130 mV was almost 1·0 at the steady state in 400 mM-Li, Na-free solution and the microscopic transition between open and closed state was expected to be negligible. By contrast, in 400 mM-Na

inactivation was clearly observed (Fig. 9*A*, inset) and the open probability of the channel at −130 mV was about 0·7 at the steady state (s_∞ = 0·7 estimated from the s_∞-potential diagram in Fig. 9*A*). On the microscopic level, the ergodic theorem says that each channel is considered to be open 70 % of the time (Lee, 1960). These microscopic open–close transitions of the channel in Na-containing medium are reflected in the steady-state current noise, resulting in a $1/[1+(f/f_c)^2]$ type p.d.s., whereas in Na-free 400 mM-Li solution a $1/f$ type p.d.s. was observed at −130 mV (Fig. 9*B*). The steady-state currents were almost identical in both solutions (−1·78

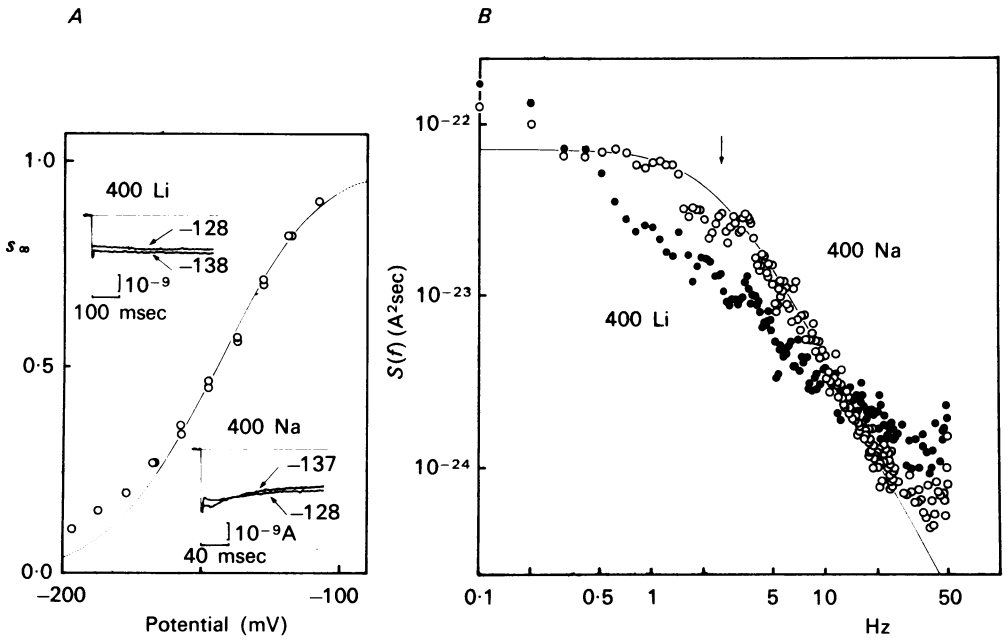

Fig. 9. Changes in inactivation process and in power density spectrum of steady-state current noise following replacement of Na with Li. *A*, s_∞-potential curve in 400 mM-Na. V_s = −145 mV, b = 19 mV. Insets show inward currents in 400 mM-Na and in 400 mM-Li solution. *B*, p.d.s. of steady-state current noise at −130 mV in 400 Na (○) and in 400 Li (●). I_∞ = −1·80 nA, s_∞ = 0·67, f_c = 2·48, γ = 8·1 pmho, N = 3700, for 400 Na. In 400 Li, a $1/f$ patterned spectrum was detected, I_∞ = −1·78 nA. Solutions F and G, buffered by 10 mM-PIPES (pH = 6·9).

and −1·80 nA in 400 Li and 400 Na solution, respectively). These results confirm that the current noise having the $1/[1+(f/f_c)^2]$ spectral pattern originates in the open–close gating kinetics of the inactivation process of the anomalous rectifier.

Part III. Unit conductance and number of K anomalous rectifier channels

In part II, the steady-state current noise recorded at potentials more negative than about −120 mV was identified as originating from the fluctuations of the inactivation process at the steady state. In part III, the conductance of the unit channel and the number of channels in the egg cell membrane will be estimated from the analysis of the steady-state current noise in various ionic environments.

Microscopic and quantitative analysis of K concentration-dependent changes in the conductance. As shown in Fig. 2*B*, the chord conductance estimated from the steady-state I–V relation increases with increasing K concentration. The increase is due to an increase either in the unit conductance, or in the number of channels, or in both. Since the holding potential was shifted in a depolarized direction with increasing K concentration, there may be some effects upon the conductance due to the increased inflow of Ca ions even in 10 mM-Ca solution. However, since the Ca effect did not seem prominent except in high Ca solution and since it was difficult to record the current noise in low Ca media (less than 10 mM), the K dependency of the channel conductance was studied in 10 mM-Ca solution; only those experiments were accepted in which reversible changes were observed when the initial K concentration was restored.

Changes of the conductance in the K anomalous rectifier due to changes of K concentration have been demonstrated in other excitable membranes (Noble & Tsien, 1968; Hagiwara & Takahashi, 1974). In the starfish egg membrane (Hagiwara & Takahashi, 1974) as well as in the tunicate egg membrane (Miyazaki, Takahashi, Tsuda & Yoshii, 1974*b*) the conductance at V_K has been shown to be proportional to the square root of the external K concentration. Corresponding changes should be observed at the microscopic level by the analysis of steady-state current noise.

Respective p.d.s. data in various K concentration media can be fitted with curves drawn according to the formula

$$S(f) = \frac{2I_\infty^2(1-s_\infty)\tau_s}{s_\infty N[1+(2\pi f\tau_s)^2]}. \tag{7}$$

This formula was derived following the treatment by Hill & Chen (1972) and by Stevens (1972). The fitting was done over the experimental points between 0·4 and 5 or 10 Hz with a least squares method. As I_∞, s_∞, τ_s could be determined from the usual relaxational voltage-clamp run, the maximum number of anomalous rectifier channels that can be opened by a hyperpolarizing pulse per egg, N, was estimated from eqn. (7) and then the unit channel conductance, γ, was calculated by the equation

$$\gamma = I_\infty/Nn_\infty s_\infty(V-V_K). \tag{8}$$

In part I, n_∞ was assumed to be 1·0 in the membrane potential range more negative than about -100 mV. Note that γN is $\bar{g}$ in eqn. (1), i.e. the maximum chord conductance.

The means of γ and N, estimated at each membrane potential and their averages are presented in Table 2. Although slight variations were observed in γ and N, no systematic changes occurred in association with the changes in membrane potential. Both the unit and maximum chord conductances changed according to the square root of the K concentration, whereas N remained almost constant. Thus, the K-dependent conductance change is due to the property of the open unit channels and not due to changes of the maximum number of channels opened by the hyperpolarizing pulse.

As the estimated value of V_K differed from cell to cell even in Na-free media, for convenience, V_K was calculated by the Nernst equation assuming $[K]_i = 260$ mM. Although this assumption results in an error in the estimation of γ, the error must be less than 5 % of γ even in 25 mM-K media, because the current noise having the $1/[1+(f/f_c)^2]$ spectrum was usually measured at

a potential more negative than −120 mV and the error in V_K estimation was less than 3 mV. This is much less than the statistical error for the estimation of the power density spectrum (see Methods).

Temperature dependency of unit channel. As described in part I the temperature coefficient (Q_{10}) for the inactivation time constant (τ_s) was 3·41 and that for the chord conductance was 1·44. The Q_{10} for the unit channel conductance was also

TABLE 2. Effect of K concentration (mM) on conductance (mean ± S.E.)

K concn. (mM)	$<\bar{g}>$ ($\times 10^{-8}$ mho)	n	Averaged		Mean γ, [N] at each membrane potential (mV)			
			N	γ	−120	−130	−140	−150
25	4·25	9	8200 ± 510	4·40 ± 0·21	4·92 [7900]	4·21 [7860]	4·34 [8100]	3·95 [9160]
50	6·12	17	8570 ± 680	5·97 ± 0·26	6·32 [8180]	5·60 [8450]	5·85 [8510]	6·30 [8310]
100	9·81	19	7930 ± 200	8·37 ± 0·32	8·61 [8030]	8·03 [8190]	8·67 [7470]	7·34 [8030]
200	12·47	13	8630 ± 900	10·33 ± 0·41	10·33 [8890]	9·79 [7180]	11·03 [9260]	—

$<\bar{g}>$, mean of the maximum chord conductances obtained from relaxational voltage-clamp run.
n, number of trials.
N, averaged number of K anomalous rectifier channels per egg.
γ, unit-conductance of K anomalous rectifier channel ($\times 10^{-12}$ mho).

estimated by the p.d.s. analysis of the steady-state current noise. Fig. 10*A* illustrates two p.d.s.s at 5 and 15 °C. The spectrum at 5 °C was multiplied by 0·9 to adjust the low frequency asymptote to that at 15 °C. The spectra were recorded at −120 mV from two egg cells in the standard solution. The spectrum shifted towards higher frequencies with a temperature increase from 5 to 15 °C. The cut-off frequency marked by arrows was 0·4 and 1·7 Hz at 5 and 15 °C, respectively. τ_N was calculated from the cut-off frequency in a number of egg cells and plotted on a log scale against temperature in Fig. 10*B* for the potential levels of −120 (○), −130 (△) and −140 mV (□). The Q_{10} of τ_N was 3·22 in the range from 5 to 20 °C, irrespective of the membrane potential, i.e. almost the same as that obtained from the relaxational runs.

The unit conductances were plotted on a log scale against temperature in Fig. 10*B* with filled symbols. The Q_{10} was 1·52 in the temperature range from 5 to 20 °C, i.e. almost the same as that of the maximum chord conductance estimated by the relaxational voltage clamp. Therefore, the temperature-dependent increase in the chord conductance was mainly due to the property of the unit channels, and not due to changes in the number of channels.

Microscopic interpretation of Ca and Mg effects upon the anomalous rectifier channel. As described in part I, a Ca dependent increase of the K conductance was observed and intracellular Ca ions may play an essential role in the Ca effects. The role of Ca in altering the unit conductance of the anomalous rectifier channels or the number of channels was also investigated using the p.d.s. technique.

The unit conductance and the number of channels were estimated for various Ca concentrations, and are presented in Table 3. The unit conductance was almost constant in 50 mM-K solution with various Ca concentrations. Unit conductances were around $6{\cdot}2 \times 10^{-12}$ mho and were similar to the value obtained in standard solution as presented in Table 2 (50 mM-K). Thus, the unit conductance is not affected by Ca ions. Consequently the maximum number of channels (N) that can be opened by a hyperpolarizing pulse must be affected by Ca ions because the maximum chord conductance was enhanced by Ca (Fig. 5*A*). However, the mean value of N, from various eggs, does not show the predicted systematic increase (Table 3).

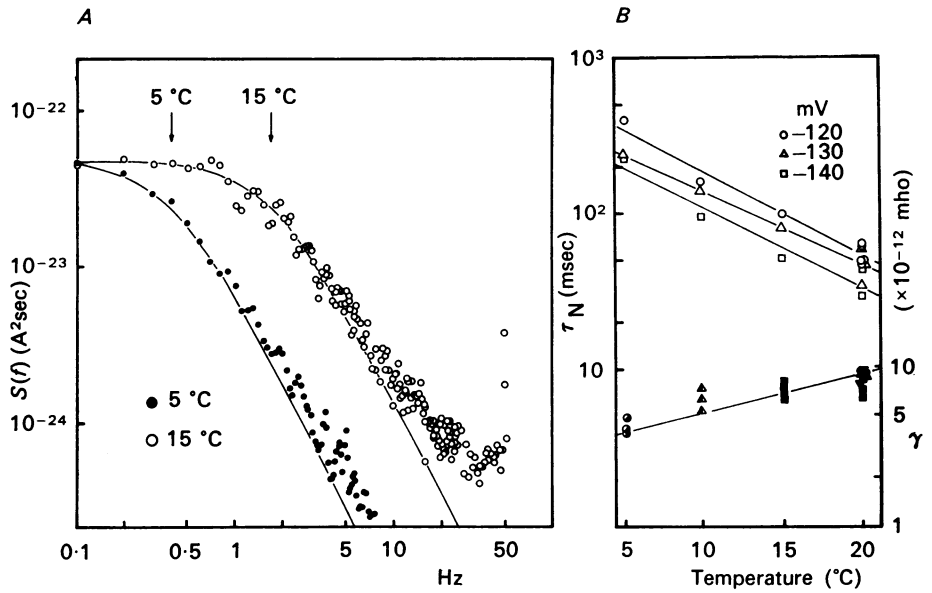

Fig. 10. Temperature dependency of current noise. *A*, p.d.s. of current noise at 5 °C (●) and at 15 °C (○) recorded at −120 mV from different cells. P.d.s. at 5 °C was multiplied by 0·9. For 5 °C, $I_\infty = -0{\cdot}83$ nA, $s_\infty = 0{\cdot}76$, $f_c = 0{\cdot}4$ Hz, $\gamma = 4{\cdot}1$ pmho, $N = 3340$. P.d.s. at 15 °C is the same as in Fig. 7. τ_N ($= 1/2\pi f_c$) (upper lines at −120 (○), −130 (△) and −140 (□) (mV), left ordinate) and γ (lower line, right ordinate) are plotted on a log scale against temperature. For γ, different symbols mean different cells. The temperature coefficient (Q_{10}) between 5 °C and 20 °C was 3·22 and 1·52 for τ_N and γ, respectively. Solutions A and B (50 mM-K).

TABLE 3. Effect of Ca concentration (mM) on γ and N (mean ± S.E.)

Ca concn. (mM)	n	γ ($\times 10^{-12}$ mho) Mean	γ CNH-139	N Mean	N CNH-139
10	7 (3)	6·15 ± 0·17	(6·46)	5451 ± 240	(4860)
20	(4)	—	(6·43)	—	(5460)
50	32 (4)	6·24 ± 0·17	(6·17)	5070 ± 270	(6580)
100	(4)	—	(5·94)	—	(8140)
200	14 (4)	6·22 ± 0·17	(6·52)	6530 ± 550	(8170)
10*	(4)	—	(6·44)	—	(8880)

* Measurement after exposure to 200 mM-Ca solution.
Parenthesized numbers were obtained from the same cell, CNH-139.

Different eggs were used for every concentration of Ca, so that individual variations between eggs might obscure the expected increase. In Table 3, data from a successive series of experiments obtained from one egg are presented in parentheses. In this experiment, noise recordings were exceptionally stable and long lasting. The $I-V$ relations from the same egg are also illustrated in Fig. 5*A*. Although the number of records was small in this series, the unit conductance was found to be constant, independent of Ca concentration. However, the number of channels increased monotonously as the Ca concentration increased. The changes in channel number were proportional to those observed in the maximum chord conductance estimated from $I-V$ relations (Fig. 5*A*). The ratio of the number of channels in 10 mM-Ca media before and after (marked with *) exposure to 200 mM-Ca solution was 1·83, which is almost equal to that of the maximum conductance ratio (1·8) in the same egg cell.

TABLE 4. Effects of Ca and Mg concentration (mM) on γ and N (mean ± S.E.)

Ca, Mg concn. (mM)		n	γ ($\times 10^{-12}$ mho)	N
50	—	8	5·92 ± 0·45	5020 ± 760
50	150	8	5·07 ± 0·17	5440 ± 410
200	—	11	6·30 ± 0·25	5650 ± 310
50*	—	8	6·04 ± 0·26	5800 ± 330
50*	150*	7	5·61 ± 0·28	7080 ± 450
100*	100*	4	5·65 ± 0·42	8170 ± 590

* Measurement after exposure to 200 mM-Ca solution.

The increase in chord conductance by Ca ions was a'so observed in the presence of Mg ions as shown in Fig. 5*C*. Mg ions were added to the solution by replacing Ca ions and keeping the total divalent cation concentration constant. Mg ions, in contrast to Ca, did not increase the conductance, but reduced it slightly. By examining the steady-state current noise, the number of channels and the unit conductances in the presence of Mg ions were estimated and are presented in Table 4. Comparing the number of channels before and after exposure to 200 mM-Ca shows a significant increase regardless of the presence of Mg ions. However, the unit conductance was slightly reduced by Mg ions. This reduction was independent of the Ca action observed in high Ca solutions. The decrease in the maximum chord conductance in the $I-V$ relations from relaxational voltage-clamp runs is mostly explained by this reduction of the unit conductance (Fig. 5*C*) and Table 4.

In conclusion, Ca ions, probably in the intracellular compartment, seem to be effective in increasing the maximum number of anomalous rectifier channels that can be opened by a hyperpolarizing pulse, and this effect is independent of the presence of Mg ions. Mg ions, on the other hand, seem to suppress the unit conductance of the channels.

DISCUSSION

In the present experiments, anomalous rectification, as described in the striated muscle membrane of the frog, was analysed in the egg cell membrane of the tunicate. The K inward current through the anomalous rectifier showed activation and in-

activation when a step potential change was applied to the membrane under voltage-clamp condition. The inactivation was found to follow first order kinetics. The simplicity of the kinetic process and the presence of a fairly large net steady-state current is convenient for noise analysis of the ionic currents related to the excitability of the membrane.

The noise analysis of the steady-state current has been useful in differentiating the unit process underlying the potential-dependent current flow through excitable membranes. The steady-state inward K current through the anomalous rectifier in the egg cell membrane showed marked fluctuations when the membrane was hyperpolarized. This current noise was identified as originating in the fluctuations of the inactivation process of the anomalous rectifier for the following reasons. (1) The spectral pattern of the p.d.s. showed only one cut-off frequency, and had the form $1/[1+(f/f_c)^2]$. This suggests a process that follows first order kinetics as the origin of the current noise at the steady state. (2) The cut-off frequency of the spectrum varied with changes in the membrane potential. (3) The p.d.s. pattern was transformed to a $1/f$ form when the potential was held at -90 mV, where the channel open probability in the steady state estimated from the relaxational voltage-clamp runs was 1·0 and no open–close transitions of each channel state were expected. (4) The transformation of the p.d.s. from the $1/[1+(f/f_c)^2]$ type to the simple $1/f$ type was also observed at the same membrane potential and with a similar amount of steady-state inward current when Na was replaced by Li; the transformation was related to the disappearance of inactivation in the Na-free solution (Fig. 9*A*, inset). Therefore, neither the membrane potential nor the membrane current itself was responsible for the generation of a $1/[1+(f/f_c)^2]$ patterned spectrum, but the presence of open–close transitions of each channel state was the cause of this spectral pattern. (5) There was a good correlation between the time constant derived from the noise analysis and that estimated from the step change of the potential. This suggests that the current noise originates in fluctuations of the inactivation gate in each channel.

The mean number of N is 6400, calculated from a total of 191 records (thirty-five cells). Thus, the mean anomalous rectifier channel density in the tunicate egg membrane is $0{\cdot}028/\mu m^2$ taking the egg diameter as 270 μm. This value is very small compared with the proposed values in other species for delayed K or for Na channels. They are $40–70/\mu m^2$ for the delayed K channel in squid giant axons (Conti *et al.* 1975), $13–35/\mu m^2$ for the Na channel in lobster giant axons (Moore, Narahashi & Shaw, 1967; Keynes, Ritchie & Rojas, 1971), $483–553/\mu m^2$ for the Na channel in squid giant axons (Levinson & Meves, 1975; Conti *et al.* 1975; Keynes & Rojas, 1976) and about $2000/\mu m^2$ for the Na channel in frog myelinated nerve fibres (Conti *et al.* 1976*b*). The current density of the tunicate egg is also very small, especially for the anomalous rectifier ($1{\cdot}27\ \mu A/cm^2$ for the peak steady-state inward K current in standard solution). This is roughly 1/1000 of the delayed K current in the squid giant axon. The channel density is also 1/1000 of the delayed K channel density in the squid giant axon as described above. However, the unit channel conductance was almost equal to that estimated for the ionic channels in other species, i.e. in the order of 10^{-12}–10^{-11} mho. For the delayed K channels of the squid giant axon, Armstrong (1975) has estimated the value of unit conductance as 3×10^{-12} mho per

channel which is in fairly good agreement with the values presented in this paper (Tables 2–4).

I would like to thank the reviewing Editor of the Journal for his comments and for improving the manuscript. It is my pleasure to express my acknowledgement to Dr K. Takahashi for his valuable advices at all stages of this work. I also thank Professor A. Takeuchi, Drs S. Miyazaki, S. Ozawa, and R. Schor for reading the manuscript and offering many valuable suggestions. I thank Professor H. Shimazu for his constant encouragement. This work was supported by a grant from the Ministry of Education, Science and Culture, Japan.

REFERENCES

ADRIAN, R. H. & FREYGANG, W. H. (1962). The potassium and chloride conductance of frog muscle membrane. *J. Physiol.* **163**, 61–103.

ALMERS, W. (1972*a*). Potassium conductance changes in skeletal muscle and the potassium concentration in the transverse tubules. *J. Physiol.* **225**, 33–56.

ALMERS, W. (1972*b*). The decline of potassium permeability during extreme hyperpolarization in frog skeletal muscle. *J. Physiol.* **225**, 57–83.

ANDERSON, C. R. & STEVENS, C. F. (1973). Voltage clamp analysis of acetylcholine produced end-plate current fluctuations at frog neuromuscular junction. *J. Physiol.* **235**, 655–691.

ARMSTRONG, C. M. (1975). Potassium pores of nerve and muscle membranes. *Membranes. A Series of Advances*, vol. 3, chap. 5, ed. EISENMAN, G., pp. 325–359. New York: Marcel Dekker, Inc.

BAKER, P. E., HODGKIN, A. L. & RIDGWAY, E. B. (1971). Depolarization and calcium entry in squid giant axons. *J. Physiol.* **218**, 709–755.

BENDAT, J. S. & PIERSOL, A. G. (1971). *Random data. Analysis and Measurement Procedures.* New York: Wiley Interscience.

BERGMAN, C. (1970). Increase of sodium concentration near the inner surface of the nodal membrane. *Pflügers Arch.* **317**, 287–302.

BEZANILLA, F. & ARMSTRONG, C. M. (1972). Negative conductance caused by entry of sodium and cesium ions into the potassium channels of squid axons. *J. gen. Physiol.* **60**, 588–608.

CONTI, F., DE FELICE, L. J. & WANKE, E. (1975). Potassium and sodium ion current noise in the membrane of the squid giant axon. *J. Physiol.* **248**, 45–82.

CONTI, F., HILLE, B., NEUMCKE, B., NONNER, W. & STÄMPFLI, R. (1976*a*). Measurement of the conductance of the sodium channel from current fluctuations at the node of Ranvier. *J. Physiol.* **262**, 699–727.

CONTI, F., HILLE, B., NEUMCKE, B., NONNER, W. & STÄMPFLI, R. (1976*b*). Conductance of the sodium channel in myelinated nerve fibres with modified sodium inactivation. *J. Physiol.* **262**, 729–742.

HAGIWARA, S., MIYAZAKI, S. & ROSENTHAL, N. P. (1976). Potassium current and the effect of cesium on this current during anomalous rectification of the egg cell membrane of a starfish. *J. gen. Physiol.* **67**, 621–638.

HAGIWARA, S. & TAKAHASHI, K. (1974). The anomalous rectification and cation selectivity of the membrane of a starfish egg cell. *J. Membrane Biol.* **18**, 61–80.

HILL, T. L. & CHEN, Y. D. (1972). On the theory of ion transport across the nerve membrane. VI. Noise from the open close kinetics of K^+ channels. *Biophys. J.* **12**, 948–959.

HODGKIN, A. L. & HUXLEY, A. F. (1952). A quantitative description of membrane currents and its application to conduction and excitation in nerve. *J. Physiol.* **117**, 500–544.

HOOGE, F. N. & GAAL, J. L. M. (1971). Fluctuations with a $1/f$ spectrum in the conductance of ionic solutions and in the voltage of concentration cells. *Philips Res. Rep.* **26**, 77–90.

HOOGE, F. N. (1972). Discussion of recent experiments on $1/f$ noise. *Physica* **60**, 130–144.

ISENBERG, G. (1975). Is potassium conductance of cardiac Purkinje fibres controlled by $[Ca^{2+}]_i$? *Nature, Lond.* **253**, 273–274.

KATZ, B. (1949). Les constantes electriques de la membrane du muscle. *Arch. Sci. physiol.* **3**, 285–300.

KEYNES, R. D., RITCHIE, J. M. & ROJAS, E. (1971). The binding of tetrodotoxin to nerve membranes. *J. Physiol.* **213**, 235–254.

KEYNES, R. D. & ROJAS, E. (1976). The temporal and steady-state relationships between activation of the sodium conductance and movement of the gating particles in the squid giant axon. *J. Physiol.* **255**, 157–189.

KRNJEVIČ, K. & LISIEWICZ, A. (1972). Injections of calcium ions into spinal motoneurones. *J. Physiol.* **225**, 363–390.

LEE, Y. W. (1960). *Statistical Theory of Communication.* New York, London: Wiley.

LEVINSON, S. R. & MEVES, H. (1975). The binding of tritiated tetrodotoxin to squid giant axons. *Phil. Trans. R. Soc.* B **270**, 349–352.

MEECH, R. W. & STANDEN, N. B. (1975). Potassium activation in *Helix aspersa* neurons under voltage clamp: a component mediated by calcium influx. *J. Physiol.* **249**, 211–239.

MIYAZAKI, S., TAKAHASHI, K. & TSUDA, K. (1974*a*). Electrical excitability in the egg cell membrane of the tunicate. *J. Physiol.* **238**, 37–54.

MIYAZAKI, S., TAKAHASHI, K., TSUDA, K. & YOSHII, M. (1974*b*). Analysis of non-linearity observed in the current–voltage relation of the tunicate embryo. *J. Physiol.* **238**, 55–77.

MOORE, J. W., NARAHASHI, T. & SHAW, T. I. (1967). An upper limit to the number of sodium channels in nerve membrane? *J. Physiol.* **188**, 99–105.

NOBLE, D. & TSIEN, R. W. (1968). The kinetics and rectifier properties of the slow potassium current in cardiac Purkinje fibres. *J. Physiol.* **195**, 185–214.

OHMORI, H. & YOSHII, M. (1977). Surface potential reflected in both gating and permeation mechanisms of sodium and calcium channels of the tunicate egg cell membrane. *J. Physiol.* **267**, 429–463.

OKAMOTO, H., TAKAHASHI, K. & YOSHII, M. (1976*a*). Membrane currents of the tunicate egg under the voltage-clamp condition. *J. Physiol.* **254**, 607–638.

OKAMOTO, H., TAKAHASHI, K. & YOSHII, M. (1976*b*). Two components of the calcium current in the egg cell membrane of the tunicate. *J. Physiol.* **255**, 527–561.

STEVENS, C. F. (1972). Inferences about membrane properties from electrical noise measurements. *Biophys. J.* **12**, 1028–1047.

VERVEEN, A. A. & DE FELICE, L. J. (1974). Membrane noise. *Prog. Biophys. molec. Biol.* **28**, 189–265.

VERVEEN, A. A. & DERKSEN, H. E. (1965). Fluctuations in membrane potential of axons and the problem of coding. *Kybernetik* **2**, 152–160.

VERVEEN, A. A. & DERKSEN, H. E. (1968). Fluctuation phenomena in nerve membrane. *Proc. IEEE* **56**, 906–916.